ACS APPLIED POLYMER MATERIALS

Letter

pubs.acs.org/acsapm

Evaluating Mechanical Properties of Polymers at the Nanoscale Level via Atomic Force Microscopy−Infrared Spectroscopy

Jehan Waeytens,[†,‡,§] Thomas Doneux,[‡] and Simone Napolitano*[,§]

[†]ExxonMobil Chemical Europe Incorporated, Hermeslaan 2, B-1831 Machelen, Belgium

[‡]Chimie Analytique et Chimie des Interfaces, Faculté des Sciences, Université libre de Bruxelles (ULB), CP 255, Boulevard du Triomphe, B-1050 Bruxelles, Belgium

[§]Laboratory of Polymer and Soft Matter Dynamics, Faculté des Sciences, Université libre de Bruxelles (ULB), CP 223, Boulevard du Triomphe, B-1050 Bruxelles, Belgium

Supporting Information

ABSTRACT: The characterization and the optimization of packaging materials require accessing their composition with nanometric precision. A possible solution comes from atomic force microscopy−infrared spectroscopy (AFM−IR), capable of acquiring IR spectra with a spatial resolution surpassing the limit of infrared spectroscopy by far. Differentiating polyolefins, a typical component of packaging films, is complicated by the large similarity in the infrared response of this class of materials. Here, we propose a method with which to improve domains differentiation based on the analysis of IR spectra and viscoelastic properties, extracted via a routine similar to that employed in contact-resonance AFM.

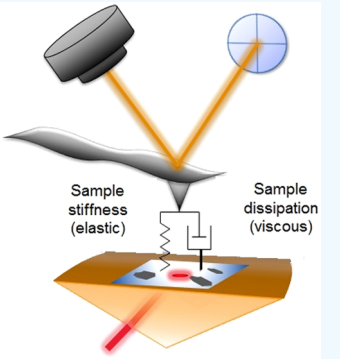

KEYWORDS: *polymers, AFM−IR, subdiffraction resolution, photothermally induced resonance*

Assembling several layers of different polymers or polymer blends is a robust method for fabricating packaging films with excellent mechanical and barrier properties. Further improvements are achieved by dispersing organic and inorganic fillers within the polymer layers, which yields a neat reduction in production costs and allows the fine-tuning of the opacity of the protective films. Because the final performance of these hybrid materials depends on a large number of parameters, e.g., the morphology of the different phases, the thickness (approximately a few hundreds of nanometers), and the composition of the single layers and the width of the interfaces, the use of several advanced techniques is commonly required.

A robust solution for the characterization of multilayers could come from atomic force microscopy−infrared spectroscopy (AFM−IR), an emerging analytical tool that allows us to combine morphological analysis via atomic force microscopy and composition by means of infrared spectroscopy in one compact setup.[1−3] IR spectra are obtained via a photothermally induced resonance (PTIR),[4] relying on the mechanical detection of the thermal expansion induced in the sample by the absorption of infrared light.

Living cells,[5] viruses and bacteria,[6,7] polymers,[8] quantum dots,[9] plasmonic nanostructures,[10] metal−organic frameworks,[11] tissues,[12] and perovskite photovoltaic devices[13] are a few examples of the large class of materials that have already been investigated with this technique. With a penetration depth exceeding 1 μm[14,15] and a spatial resolution of ∼20 nm,[16] well below the diffraction limit of the IR beam (∼5 μm), AFM−IR could soon become a standard technique that allows the reverse engineering of multilayer films.[17]

One crucial limitation of the technique, however, severely retards the achievement of this goal: because the IR spectra of polyolefins, the major components of packaging films, are very similar, differentiation of the specific polymers remains challenging. In this regard, Tang et al. have recently proposed to differentiate polypropylene and polyethylene-*co*-propylene domains by implementing a calibration curve obtained via conventional FTIR in the analysis of AFM−IR data.[18] Such a method, although it is affected by large uncertainties (a standard deviation of ∼14% and a relative error of ∼20%), permitted a differentiation between PP matrix and part of the nanoscale inclusions.

Here, we introduce an analytical methodology, based on the measurement of viscoelastic properties, to improve differentiation of polyolefins via AFM−-IR. Our method exploits the huge impact on mechanical properties induced by small variations in co-monomer contents. We extract a mechanical response from the time dependence of the IR signal at the cantilever and sample contact, allowing the nanometric spatial

Received: December 18, 2018
Accepted: December 28, 2018
Published: December 28, 2018

DOI: 10.1021/acsapm.8b00243
ACS Appl. Polym. Mater. XXXX, XXX, XXX−XXX

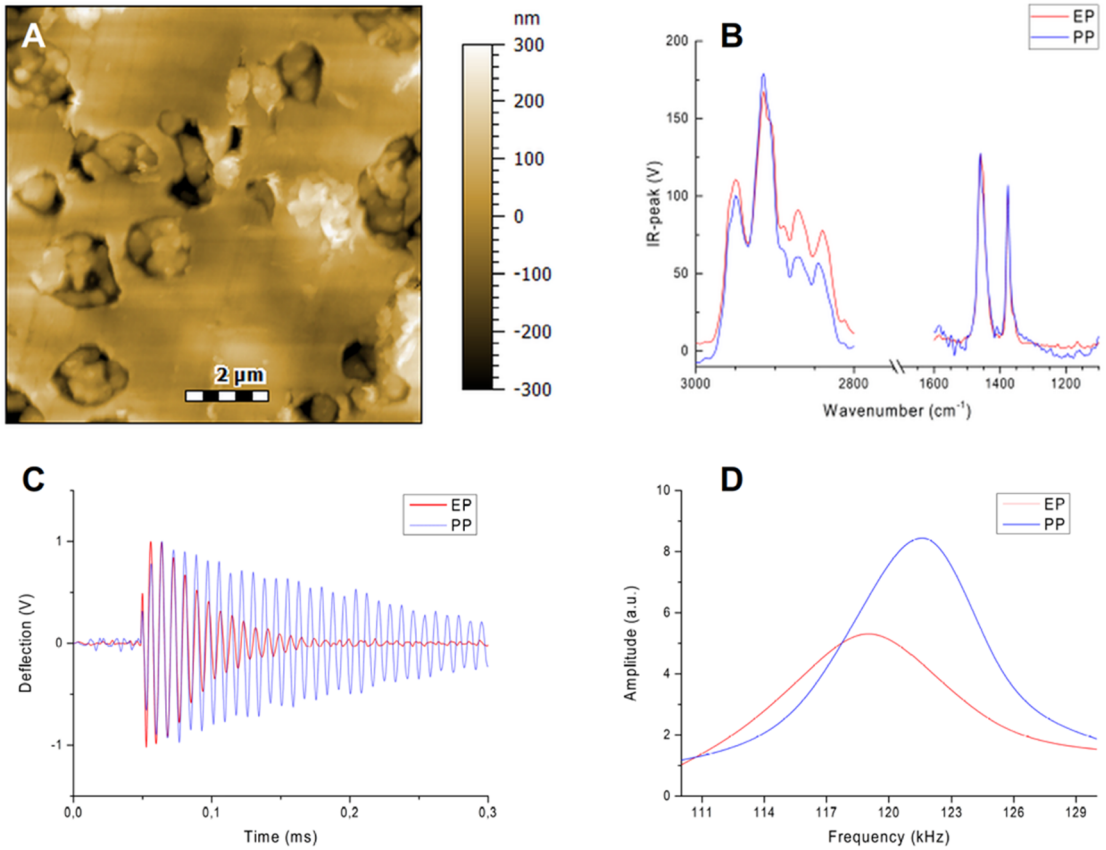

Figure 1. (A) Topography image, at constant load, of a cross-section of ICP obtained with the ThermaLever. The colored circles indicate the locations (blue for PP and red for EP) of the acquisition done at 1460 cm^{-1} with a laser power of 10% (B) AFM-IR spectra at the two locations. (C) Deflection signal(IR peak). (D) FT of the deflection signals (IR amplitude).

resolution of components having almost-identical IR spectra. Our strategy is based on the contact resonance (CR-AFM) technique,[19] a standard AFM working mode, in which the cantilever oscillates in contact with the sample while scanning over the surface; see Figure 1. To understand how the cantilever interacts with the polymer surface, we considered an equivalent mechanical circuit widely used to reproduce the viscoelastic response of polymers, corresponding to a viscous damper in parallel with an elastic spring (the Kelvin−Voigt model).[20]

The analysis of resonances in the amplitude of the deflection induced in the tip allows the extraction of information regarding the viscoelastic properties of the surface. A shift in the resonance frequency of the cantilever provides information on the sample stiffness, parametrized via the elastic constant of the spring considered in the Kelvin−Voigt model. The energy dissipation or damping is, instead, proportional to the quality (Q) factor of the resonance (a dimensionless factor that describes how damped an oscillator is). The latter parameter corresponds to the amplitude of the cantilever at the resonance frequency or, equivalently, to the full width at half height of the resonance peak. A quantitative characterization of viscoelastic properties with nanometric resolution is, hence, possible by simply fitting the value of resonance peaks found for each position (pixel) scanned on the surface of the sample to a simple mechanical model.

Considering the large analogy between PTIR and CR-AFM, we expect that AFM−IR could also be used to probe physical properties and molecular properties down to the nanoscale level. Although full achievement of this goal would require the introduction of a more robust theoretical framework, we propose here that the sensitivity of AFM−IR to mechanical properties could be exploited to differentiate materials domains having almost-identical IR spectra.

To verify our claims, we considered a copolymer of polypropylene (ICP) composed of a rigid matrix of polypropylene (PP) with ethylene−propylene rubber (EPR) inclusions. Investigation via traditional IR spectroscopy of this material, commonly used in packaging films, would not allow the mapping of the distribution and the size of the different domains because those are well below the diffraction limit.

In AFM−IR, similar to an attenuated total reflection (ATR) setup, the IR beam here reflects on the sample sitting on a ZnSe prism with a pulse of 12 n, at the rate of 1 pulse per millisecond. The induced evanescent wave diffuses across the whole polymer layer, which rises the temperature and, hence, increases the sample thickness. Because the tip was already in contact with the sample, the sudden change in the height of the surface induces an instantaneous deflection in the cantilever. This excitation eventually decays upon interaction with the polymer layer and provides a straightforward way to probe the viscoelastic properties of the surface. Although we used a conventional tip with relatively low characteristic resonance frequency (120.5 kHz),[21] the measurement is not affected by time-dependent variations in the surface height, decaying at the time scale of heat relaxation ($\lesssim 1\ \mu s$). We remark that in the case of AFM−IR, the deflection signal does not convolute with

DOI: 10.1021/acsapm.8b00243
ACS Appl. Polym. Mater. XXXX, XXX, XXX−XXX

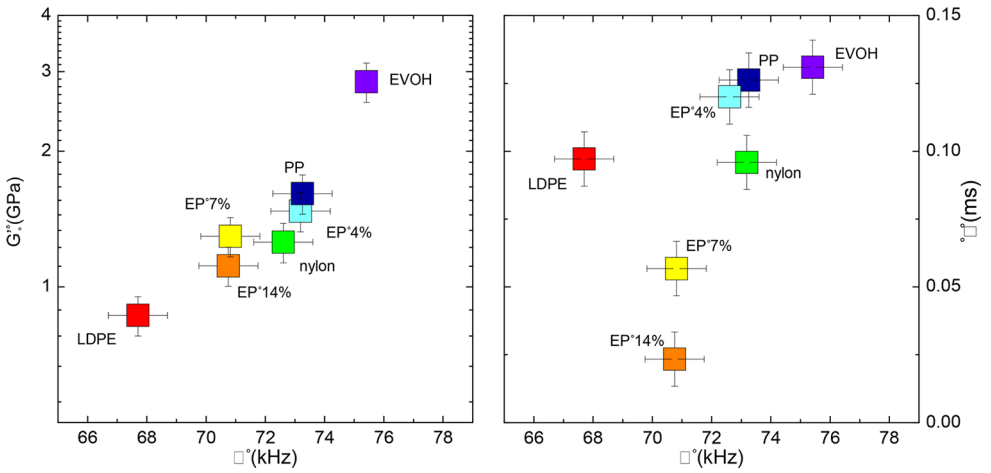

Figure 2. Left panel shows the correlation between the frequency and the storage modulus G' at 223 K. Data were obtained at 1460 cm^{-1} with a contact tip from Anasys Instruments and with a load force of 37.5 nN. The right panel shows the differentiation of materials with close frequencies based on the decay time. Data were obtained at 1460 cm^{-1} with a contact tip from Anasys Instruments and with a load force of 37.5 nN.

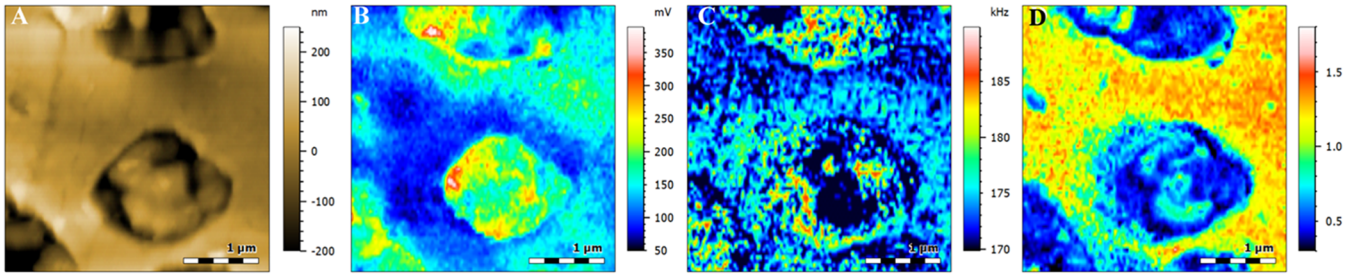

Figure 3. Images of a cross-section of ICP obtained with the ThermaLever. (A) Topography image. (B) IR peak map. (C) Resonance frequency map. (D) Map of the dimensionless ratio I_ω/A_0, where I_ω is the amplitude of the Fourier-transformed IR signal at its resonance frequency and A_0 is the deflection at zero time. The maps were obtained at 1460 cm^{-1} with a laser power of 8% at an acquisition rate of 0.05 Hz with a pulse co-averaging of 32 scans.

thermal expansivity because its off-resonance sensitivity is low.[22]

The deflection in the cantilever with respect to the surface can be described as the sum of damped harmonic oscillators of the following type:[23]

$$S = A_0 \cos(\omega t) \exp\left(-\frac{t}{\tau}\right) \quad (1)$$

where A_0 is the deflection at zero time, ω is the frequency of the selected (a pass-band filter was used) eigenmode, and τ its characteristic decay time. ω is directly related to the shift in frequency of the cantilever and, thus, to the stiffness of the sample (parametrized, for example, by the elastic modulus G'), while τ provides information on the viscous character of the material (loss modulus G''). In fact, the Fourier transformation of the expression in eq 1 provides a Lorentzian function centered at ω. The value of τ can be straightforwardly obtained as $(a\pi)^{-1}$, where a is the full width at half height of the transformed signal,[13] related to the damping component of our mechanical circuit.

Figure 1A shows the topography image obtained in contact mode on a section of ICP, where inclusions of EPR, darker on the image, are dispersed in the PP matrix. In Figure 1B, we report the damped oscillating signals (deflection in the cantilever with respect to the surface) measured on the polypropylene matrix and on the ethylene−propylene inclusion; the corresponding Fourier-transformed signals are plotted in Figure 1C. Although both polymers have the same maximum starting amplitude (A_0), the oscillations in the EP domain decays much faster than in the PP matrix. The first observation implies that the two polymers experienced a comparable change in volume upon thermal expansion, while the latter indicates that the EP inclusions dissipate more efficiently the thermal impulse, consistent with the rubbery character of this polymer.

To complete the validation of our claims, we performed an additional set of experiments in which we measured via dynamic mechanical thermal analysis (DMTA) the mechanical properties of different commercial polymers. Based on the work of Yablon et al., the Q factor and the resonance frequency are a probe of the viscous and elastic mechanical response.[24] To quantify these parameters, we measured the temperature and frequency response of the storage and loss modulus (G' and G''). We expect a direct correlation between ω, the shift in frequency of the cantilever, and G' (elastic response) and between G'' and τ because both quantities provide information regarding the viscous character of the material.

Although we could not reach via DMTA the high resonance frequency used in AFM−IR, simple considerations allowed us to compare the results obtained via the two experimental methods. AFM−IR was operated at room temperature at 70 kHz, associated with a characteristic time of ∼2 μs. In these conditions, all of the polymers investigated are in the glassy state and exhibit an unrelaxed mechanical solid-like response. This regime corresponds to a high modulus plateau in G' coupled to zero loss ($G'' \simeq \partial G'/\partial \log\omega$, an approximation

DOI: 10.1021/acsapm.8b00243
ACS Appl. Polym. Mater. XXXX, XXX, XXX−XXX

valid for all the dynamic complex functions owing to the Kramers−Kronig relation), as observed at low temperatures in isochronal conditions. Because of the lack of material dependence on the intrinsic value of G'' at low temperatures and high frequency, the comparison between viscoelastic properties and IR signal can be performed only for G'. We considered 223 K, the lowest temperature achievable by the DMTA setup, in which each analyzed polymer is in the glassy state. In Figure 2, we plotted the values of ω (see eq 1) measured via AFM−IR, as a function of the values of G'. The excellent correlation between two independent data sets validate our claims on the sensitivity of AFM-IR on nanoscale mechanical properties.

Despite the lack of correlation with G'', the decay time τ can be used to differentiate materials whose characteristic frequency ω is too close. Analysis of τ can be, hence, employed to overcome possible limitations of our method due to G' values that are too similar. In the left panel of Figure 2, we show that the elastic moduli of PP and EP 4% are identical within experimental errors; therefore, differentiating PP and EP by ω is not possible. On the contrary, the decay time of those materials differs significantly; see the right panel of Figure 2. The differentiation of polypropylene and poly-ethylene-*co*-propylene is, therefore, possible based on the decay time.

With these ideas in mind, in Figure 3, we show an example of analysis of the same material used in Figure 1. Contrast in the topography image (Figure 3A) is ensured by the different elastic modulus of the two components. Scanning at constant force results in apparently lower heights for softer domains, where the tip can penetrate deeper. Consequently, EP domains appear darker. This effect convolutes with IR absorption in a traditional IR map (Figure 3B), which reduces contrast between the different polymers. A more-accurate differentiation of the domains is obtained by mapping the resonance frequency (Figure 3C) or a dimensionless parameter given by the ratio of the maximum amplitude of the Fourier-transformed IR signal and the intensity of the deflection at zero time (Figure 3D). This parameter, proportional to the line width and inversely proportional to the decay time, was build up to further exploit the contrast arising from the large difference in the mechanical behavior of the two polymers.

We are confident that our viscoelastic analysis will be widely employed, in combination with IR signatures, to achieve a more-accurate analysis of polymer components in packaging films and other devices. We hope that our experimental data will stimulate discussion in the community and promote the development of a valid theoretical framework with which to obtain quantitative viscoelastic information via AFM−IR measurements.

■ ASSOCIATED CONTENT

Supporting Information

The Supporting Information is available free of charge on the ACS Publications website at DOI: 10.1021/acsapm.8b00243.

Experimental protocol followed for AFM−IR and DMTA measurements (PDF)

■ AUTHOR INFORMATION

Corresponding Author

*E-mail: snapolit@ulb.ac.be.

ORCID

Thomas Doneux: 0000-0002-9082-8826

Simone Napolitano: 0000-0001-7662-9858

Notes

The authors declare no competing financial interest.

■ ACKNOWLEDGMENTS

We thank Luc Vandendriessche and Jérome Sarrazin for performing DMTA measurements, Anton-Jan Bons and Johan Stuyver for advice on AFM measurements, and Alexandre Dazzi for fruitful discussion on AFM−IR.

■ REFERENCES

(1) Centrone, A. Infrared Imaging and Spectroscopy Beyond the Diffraction Limit. *Annu. Rev. Anal. Chem.* **2015**, *8*, 101−126.

(2) Dazzi, A.; Prater, C. B. AFM-IR: Technology and Applications in Nanoscale Infrared Spectroscopy and Chemical Imaging. *Chem. Rev.* **2017**, *117*, 5146−5173.

(3) Hinrichs, K.; Shaykhutdinov, T. Polarization-Dependent Atomic Force Microscopy-Infrared Spectroscopy (AFM-IR): Infrared Nano-polarimetric Analysis of Structure and Anisotropy of Thin Films and Surfaces. *Appl. Spectrosc.* **2018**, *72*, 817−832.

(4) Dazzi, A.; Prazeres, R.; Glotin, F.; Ortega, J. M. Local Infrared Microspectroscopy with Subwavelength Spatial Resolution with an Atomic Force Microscope Tip Used as a Photothermal Sensor. *Opt. Lett.* **2005**, *30*, 2388−2390.

(5) Mayet, C.; Dazzi, A.; Prazeres, R.; Allot, F.; Glotin, F.; Ortega, J. M. Sub-100 nm IR Spectromicroscopy of Living Cells. *Opt. Lett.* **2008**, *33*, 1611−1613.

(6) Dazzi, A.; Prazeres, R.; Glotin, F.; Ortega, J. M.; Al-Sawaftah, M.; de Frutos, M. Chemical Mapping of the Distribution of Viruses into Infected Bacteria With a Photothermal Method. *Ultramicroscopy* **2008**, *108*, 635−641.

(7) Deniset-Besseau, A.; Prater, C. B.; Virolle, M.-J.; Dazzi, A. Monitoring TriAcylGlycerols Accumulation by Atomic Force Microscopy Based Infrared Spectroscopy in Streptomyces Species for Biodiesel Applications. *J. Phys. Chem. Lett.* **2014**, *5*, 654−658.

(8) Kelchtermans, M.; Lo, M.; Dillon, E.; Kjoller, K.; Marcott, C. Characterization of a Polyethylene−Polyamide Multilayer Film using Nanoscale Infrared Spectroscopy and Imaging. *Vib. Spectrosc.* **2016**, *82*, 10−15.

(9) Sauvage, S.; Driss, A.; Réveret, F.; Boucaud, P.; Dazzi, A.; Prazeres, R.; Glotin, F.; Ortéga, J. M.; Miard, A.; Halioua, Y.; Raineri, F.; Sagnes, I.; Lemaître, A. Homogeneous Broadening of the *S* to *P* Transition in InGaAs/GaAs Quantum Dots Measured by Infrared Absorption Imaging with Nanoscale Resolution. *Phys. Rev. B: Condens. Matter Mater. Phys.* **2011**, *83*, 035302.

(10) Katzenmeyer, A. M.; Chae, J.; Kasica, R.; Holland, G.; Lahiri, B.; Centrone, A. Nanoscale Imaging and Spectroscopy of Plasmonic Modes with the PTIR Technique. *Adv. Opt. Mater.* **2014**, *2*, 718−722.

(11) Katzenmeyer, A. M.; Canivet, J.; Holland, G.; Farrusseng, D.; Centrone, A. Assessing Chemical Heterogeneity at the Nanoscale in Mixed-Ligand Metal−Organic Frameworks with the PTIR Technique. *Angew. Chem., Int. Ed.* **2014**, *53*, 2852−2856.

(12) Marcott, C.; Lo, M.; Kjoller, K.; Fiat, F.; Baghdadli, N.; Balooch, G.; Luengo, G. S. Localization of Human Hair Structural Lipids Using Nanoscale Infrared Spectroscopy and Imaging. *Appl. Spectrosc.* **2014**, *68*, 564−569.

(13) Yuan, Y.; Chae, J.; Shao, Y.; Wang, Q.; Xiao, Z.; Centrone, A.; Huang, J. Photovoltaic Switching Mechanism in Lateral Structure Hybrid Perovskite Solar Cells. *Adv. Energy Mater.* **2015**, *5*, 1500615.

(14) Lahiri, B.; Holland, G.; Centrone, A. Chemical Imaging Beyond the Diffraction Limit: Experimental Validation of the PTIR Technique. *Small* **2013**, *9*, 439−445.

(15) Ramer, G.; Aksyuk, V. A.; Centrone, A. Quantitative Chemical Analysis at the Nanoscale Using the Photothermal Induced Resonance Technique. *Anal. Chem.* **2017**, *89*, 13524−13531.

DOI: 10.1021/acsapm.8b00243
ACS Appl. Polym. Mater. XXXX, XXX, XXX−XXX

(16) Katzenmeyer, A. M.; Holland, G.; Kjoller, K.; Centrone, A. Absorption Spectroscopy and Imaging from the Visible through Mid-Infrared with 20 nm Resolution. *Anal. Chem.* **2015**, *87*, 3154−3159.
(17) Eby, T.; Gundusharma, U.; Lo, M.; Sahagian, K.; Marcott, C.; Kjoller, K. Reverse Engineering of Polymeric Multilayers using AFM-based Nanoscale IR Spectroscopy and Thermal Analysis. *Spectroscopy Europe* **2012**, *24*, 18−21.
(18) Tang, F.; Bao, P.; Su, Z. Analysis of Nanodomain Composition in High-Impact Polypropylene by Atomic Force Microscopy-Infrared. *Anal. Chem.* **2016**, *88*, 4926−4930.
(19) Yamanaka, K.; Ogiso, H.; Kolosov, O. Analysis of Subsurface Imaging and Effect of Contact Elasticity in the Ultrasonic Force Microscope. *Jpn. J. Appl. Phys.* **1994**, *33*, 3197.
(20) Dinelli, F.; Ricci, A.; Sgrilli, T.; Baschieri, P.; Pingue, P.; Puttaswamy, M.; Kingshott, P. Nanoscale Viscoelastic Behavior of the Surface of Thick Polystyrene Films as a Function of Temperature. *Macromolecules* **2011**, *44*, 987−992.
(21) Dazzi, A.; Glotin, F.; Carminati, R. Theory of Infrared Nanospectroscopy by Photothermal Induced Resonance. *J. Appl. Phys.* **2010**, *107*, 124519.
(22) Chae, J.; An, S.; Ramer, G.; Stavila, V.; Holland, G.; Yoon, Y.; Talin, A. A.; Allendorf, M.; Aksyuk, V. A.; Centrone, A. Nanophotonic Atomic Force Microscope Transducers Enable Chemical Composition and Thermal Conductivity Measurements at the Nanoscale. *Nano Lett.* **2017**, *17*, 5587−5594.
(23) Dazzi, A.; Prater, C. B.; Hu, Q.; Chase, D. B.; Rabolt, J. F.; Marcott, C. AFM-IR: Combining Atomic Force Microscopy and Infrared Spectroscopy for Nanoscale Chemical Characterization. *Appl. Spectrosc.* **2012**, *66*, 1365−1384.
(24) Yablon, D. G.; Gannepalli, A.; Proksch, R.; Killgore, J.; Hurley, D. C.; Grabowski, J.; Tsou, A. H. Quantitative Viscoelastic Mapping of Polyolefin Blends with Contact Resonance Atomic Force Microscopy. *Macromolecules* **2012**, *45*, 4363−4370.

DOI: 10.1021/acsapm.8b00243
ACS Appl. Polym. Mater. XXXX, XXX, XXX−XXX